Applied Geochemistry 101 (2019) 62–74

Contents lists available at ScienceDirect

Applied Geochemistry

journal homepage: www.elsevier.com/locate/apgeochem

Corrigendum

Corrigendum to "Metallurgical slags from Cu production and Pb recovery in Poland - Their environmental stability and resource potential" [Appl. Geochem. 98 (2018) 459-472]

Bartosz Mikoda[a,*], Harry Kucha[a], Anna Potysz[b], Ewa Kmiecik[a]

[a] AGH University of Science and Technology, Faculty of Geology, Geophysics and Environmental Protection, Al. A. Mickiewicza 30, 30-059, Krakow, Poland
[b] University of Wrocław, Institute of Geological Sciences, Cybulskiego 30, 50-205, Wrocław, Poland

ARTICLE INFO

Editorial handling by Prof. M. Kersten

Keywords:
Copper slag
Lead slag
Critical elements
Resource
Environmental stability

ABSTRACT

Three different residues from Pb recovery (lead slag - LS) and Cu smelting (shaft furnace slag - SFS, and granulated slag - GS) in Cu foundries, located in the SW Poland, were examined with respect to chemical and phase composition. The examined materials reveal distinct mineral composition. The LS slag exhibits crystalline structure, and main phases observed in this slag were sulfides (nukundamite, idaite, sphalerite, troilite), spinel oxides (magnetite and chromite), intermetallic compounds (Cu, Pb and Fe) and non-stoichiometric olivines. The SFS slag and the GS slag are amorphous apart from the presence of some crystalline phases such as spinels and sulfides in the SFS sample. Both SFS and GS slags have metallic Cu and Pb inclusions. The samples are abundant in potentially toxic elements such as Cu, Pb and Zn, as well as critical elements such as REE, Co, Mo and V (up to 308, 1445, 773 and 1228 mg kg^{-1}, respectively). Two standardized leaching protocols were applied to illustrate the leaching potential of selected metal(loid)s. The slags were found chemically resistant to leaching by simulated rainfall or water. Six-step sequential extraction revealed that labile forms of metals are present in granulated slag, that exhibits mainly vitreous texture.

1. Introduction

Copper is recovered from ores mainly by means of pyrometallurgical processes that are responsible for generating waste slag, estimated at a level of ca. 2.2 tons of slag for every ton of Cu (Gorai et al., 2003; Jarošíková et al., 2017). Worldwide production of recoverable Cu reached 19.7 Mt in 2017 (USGS, 2018), and was associated with at ca 43 Mt of slags in 2017. Copper slags resemble basalt rocks from chemical and mineralogical point of view. Their chemical nature and other unique properties (sharp-edged shape, resistance to corrosion) enable utilization of slags in many ways, for example in road construction (Murari et al., 2015 and references therein) or as replacement of sand in concrete of different applications (Shi et al., 2008; Wu et al., 2010; Kua, 2013). On the other hand, these materials contain substantial amounts of potentially toxic elements. These include, Cu, Pb, Zn, As, Cd, Cr etc., which are proved to pose danger to biotic and abiotic environments (Kabata-Pendias and Szteke, 2015; Potysz et al., 2016a, 2017, 2018c). These elements can be released from the slags as the result of prolonged exposure to weathering conditions and consequently contaminate nearby ecosystems as proven in numerous studies (Piatak et al., 2004, 2015; Lottermoser, 2005; Vítková et al., 2010, 2011; Kierczak and Pietranik, 2011; Kierczak et al., 2013; Khorasanipour and Esmaeilzadeh, 2016; Kaksonen et al., 2017; Potysz et al., 2018b). Mineralogical and chemical investigations are useful not only to understand the environmental impacts of slag dumps, but also to reproduce slag formation conditions (Sãez et al., 2003; Puziewicz et al., 2007; Ettler et al., 2009; Warchulski et al., 2015; Potysz et al., 2016b; Tyszka et al., 2018).

Copper is recovered from Kupferschiefer ores located in SW Poland. In 2015, 479,000 Mg of Cu was produced (Kozłowska-Roman and Oszczepalski, 2016), which was associated with the generation of over 1 Mt of slag. Polish copper deposits contain considerable amounts of metals that are not recovered in the smelting process, e.g. REE, Co, Mo and V (Kucha, 2003; Sawłowicz, 2013; Oszczepalski et al., 2016; Sawłowicz and Sutton, 2017). These metals (except for Mo) are listed as critical raw materials for the EU (EC, 2017) because they are not

DOI of original article: https://doi.org/10.1016/j.apgeochem.2018.09.009
* Corresponding author.
E-mail addresses: bartosz.mikoda@agh.edu.pl (B. Mikoda), kucha@geol.agh.edu.pl (H. Kucha), anna.potysz@uwr.edu.pl (A. Potysz), ewa.kmiecik@agh.edu.pl (E. Kmiecik).

https://doi.org/10.1016/j.apgeochem.2018.11.017
Received 19 November 2018; Accepted 19 November 2018
Available online 25 December 2018
0883-2927/

produced from the EU resources, their availability is limited and the demand is covered by import, mostly from unstable countries, which provides high supply risk. Moreover, the use of these metals in modern technologies is constantly increasing (Du and Graedel, 2013). As a result, many exploration and recovery projects have been undertaken seeking for primary and secondary resources of these metals (Goodenough et al., 2016; Paulick and Machacek, 2017). Secondary resources can be potentially attractive sources of metals of interest if the metal recovery rate is high enough (Du and Graedel, 2011; Binnemans et al., 2013; Schulze and Buchert, 2016; Potysz et al., 2018a).

The aim of this research was to assess chemical and phase composition as well as geochemical stability of different types of slags from copper smelting facilities in SW Poland. Slag stability was assessed in lab-simulated weathering conditions. These goals were achieved by combining microscopic (reflected light microscopy, scanning electron microscopy), X-Ray diffraction and chemical studies with standardized leaching protocols and sequential extraction procedure. The comprehensive characteristic obtained during applied research provides essential answers concerning the behavior of these wastes and demonstrates future research directions.

2. Materials

Three different slag samples were collected from different parts of the copper production chain and have been characterized with respect to chemical and phase composition. The examined samples represent different steps of production and are derived from various technological processes.

Lead slag (LS) from Głogów foundry is a waste derived from Dörschl reverberatory furnace. It is generated in this Pb recovery process from different wastes, mainly dusts and slimes from flue gas cleaning and the slag from Kaldo furnace (Muszer, 2006). These by-products applied to the process are rich in Pb to the extent that its recovery is economically viable. All above-mentioned wastes used in lead recovery process originate from copper processing; thus, LS is also classified as copper smelting by-product.

Shaft furnace slag (SFS) was derived from Legnica foundry where ore concentrates in the form of briquettes, as well as converter slag, are melted in the shaft furnace. This type of slag is representative for the shaft furnace technology, which is one of two basic Cu smelting technologies both in Poland and worldwide. The briquettes melted in the shaft furnace contain mainly concentrates from the black shale (Kupferschiefer) ore, which is the most metal-rich (e.g. Co, Mo, V, REE) part of the orebody (Kucha, 2003; Sawłowicz, 2013; Oszczepalski et al., 2016).

Granulated slag (GS) was collected from Głogów foundry. This slag is generated in a rapid water-cooling process of electric furnace residuum. This slag is the second-stage product of the copper ore enrichment. The copper concentrates in Głogów foundry are melted in flash furnace. This process is associated with the generation of Cu-rich waste slag, which serves as a feed for the electric furnace. The Cu metal recovered in the electric furnace is further processed, and the GS is being rapidly cooled with water on a heap. The granules resulting from this process are highly vitreous and sharp-edged in shape. For that reason, GS is being sold as the abrasive material.

3. Methods

3.1. Bulk chemical composition

The chemical composition of slag samples was determined using inductively coupled plasma optical emission spectrometry (ICP-OES) after lithium borate/tetraborate fusion and digestion of the melting product with nitric acid in Bureau Veritas Minerals Laboratories (formerly ACME Analytical Laboratories; Vancouver, Canada). Total sulfur and carbon contents were determined by LECO combustion (Bureau Veritas Minerals Laboratories). Loss of ignition (LOI) was determined by sample sintering at 1000 °C.

3.2. X-ray diffraction

The phase composition was determined using X-Ray powder diffraction (XRD; Rigaku MiniFlex 600 diffractometer with scintillation counter equipped with lithium iodide detector). The following settings were used for the analysis: Cu-Kα radiation, 3–75° 2Θ range, and 0.05° step. XRD data were processed using XRAYAN software coupled with JCPDS-ICDD 2013 database.

3.3. Microscopic observations

Slag samples were crushed and sieved through 1 mm sieve, collected and embedded in resin in 1-inch diameter metal rings. Subsequently, the rings were polished with 1 μm diamond polishing paste, using oil as a lubricant. The polished rings were investigated in reflected light using Nikon Eclipse LV100POL microscope. Selected areas of samples were observed using scanning electron microscope (SEM; FEI Quanta 200 FEG) coupled with EDAX energy dispersion spectrometer (EDS). Following parameters were used: low vacuum mode, 20 kV accelerating voltage, 10 nA beam current, 50 s counting time, 34° take-off angle. Total of 103 analyzes has been performed by EDS. The calculation of Fe (II) and Fe(III) in spinels was performed by charge balance.

3.4. Leaching experiments

Two standardized leaching tests were performed on all slag samples to evaluate their characteristics concerning their contamination potential. Each of the protocols was dedicated to explain the behavior of waste exposed to different environmental conditions. Both tests were performed in duplicates with procedural blanks.

European norm EN 12457 (EN 12457, 2002), transferred to Polish normative system as PN-EN 12457, was used to demonstrate potential of water to extract toxic substances from waste materials. The 1 g of each slag (fraction < 1 mm) was mixed with 10 cm^3 of distilled water (according to EN 12457–2:2002 part of protocol) and shaken on an orbital shaker for 24 h at 100 rpm.

The US EPA 1312 Test Method – Synthetic Precipitation Leaching Procedure (SPLP; US EPA, 1994) method was applied to simulate rainfall and to assess release of contaminants from waste materials, e.g. deposited on dumps or tailings (Lackovic et al., 1997). The extraction liquid consisted of distilled water, acidified to pH 4.2 ± 0.05 with mixture of sulfuric and nitric acid (60:40 wt ratio). The extracting agent in amount of 20 cm^3 was mixed with 1 g portion of each slag sample (fraction < 1 mm) and the solutions were shaken for 18 h on an orbital shaker at 100 rpm.

The geochemical forms of metals were examined using a six-step sequential extraction procedure. The procedure used in this study is a modified version of the six-step extraction proposed by Kersten and Förstner (1986). The 0.5 g portions of slag samples (< 1 mm grain size) were put in Falcon tubes and filled with extracting solution. The detailed description of liquid-to-solid ratios, extraction time and reagents used are presented in Table 1.

After leaching experiments, the solutions were centrifuged (3500 rpm, 10 min) to settle the particles. The supernatants were collected by syringes, filtered through Pureland® syringe 0.45 μm filters and acidified to pH < 2 with 0.1 cm^3 of 65% nitric acid.

The concentrations of selected elements (As, Cd, Cr, Cu, Pb, Zn) were determined using inductively coupled plasma mass spectrometry (ICP-MS) with Perkin Elmer ELAN 6100 apparatus, according to 17294–2 ISO Standard (2016). Limits of quantification were (mg dm^{-3}): 0.001 for As, Cu and Zn; 0.0003 for Cd, 0.005 for Cr and 0.0001 for Pb. Sigma-Aldrich multielement ICP standards were used as internal

Table 1
Parameters of sequential extractions with targeted fraction. Note: targeted fraction is obtained in routinely leached samples (e.g. soils); in waste materials, the dissolution of mineral phases might be slightly different.

Step	Chemical agent	pH	SSR	Conditions	Time [min]	Fraction
I	40 cm^3 1 M $C_2H_4O_2$	7	1:80	Shaking	120	Exchangeable + carbonate (F1)
II	40 cm^3 0.1 M $[NH_3OH]Cl$	2	1:80	Shaking	30	Mn oxides (F2)
III	25 cm^3 0.2 M $(NH_4)_2C_2O_4*H_2O$ + 25 cm^3 0.2 M $C_2H_2O_4*2H_2O$	3	1:100	Shaking in the dark	240	Amorphous Fe oxides (F3)
IV	35 cm^3 0.2 M $C_6H_5Na_3O_7$ + 5 cm^3 0.2 M $C_6H_8O_7$ + 0.5 g $Na_2S_2O_4$	ns	1:80	Ultrasound mixing, 45 °C	30	Crystalline Fe oxides (F4)
V	2 × 10 cm^3 30% H_2O_2			Heating (85 °C)	2 × 60	
	1 M $C_2H_7NO_2$	2	1:100	Shaking (to complete the reaction)	30	Sulfides (F5)
VI	10 cm^3 *aqua regia*	ns	1:20	Digestion (130 °C)	120	Residual (F6)

SSR - sample-to-solvent ratio; ns - not specified.

standards. Internal standards and samples were analyzed in triplicates, and the level of precision was < 5%. Calibration of the apparatus was done after every 10 analyzed samples. Randomly chosen samples were analyzed again to confirm the correctness of the analysis. Obtained results were compared to Polish environmental regulations concerning levels of metals in wastewaters (RME, 2014) and levels of metals in leachates from waste directed to dispose of at non-hazardous waste sites (RMEc, 2015).

4. Results

4.1. Chemical composition

The chemical composition varies from one type of slag sample to another (Table 2). Per major elements, main components of every sample are SiO_2, Al_2O_3, Fe_2O_3, MgO and CaO. Chemical composition of SFS is characterized by the highest concentration of SiO_2 as compared to other samples (43.72 wt%). The composition of LS and GS samples is also dominated by SiO_2, but its content is lower (33.05 and 38.27 wt%, respectively). The concentrations of Al_2O_3 (12.45 and 12.39 wt%, respectively) and MgO (6.48 and 6.33 wt%, respectively) are virtually the same in SFS and GS; LS is slightly impoverished in MgO (4.99 wt%) and notably impoverished in Al_2O_3 (5.73 wt%) compared to other two slag samples. SFS and LS samples contain the same amount of CaO (11.57 and 10.37 wt%, respectively); GS sample is rich in CaO (23.56 wt%). LS sample is also enriched in Fe_2O_3 (33.42 wt%) when compared to SFS and GS (18.91 and 11.53 wt%, respectively). Other constituents are also present in slags, but their content is below 4 wt% (Table 2). Noteworthy, LS is enriched in Cr_2O_3, MnO and total sulfur, compared to SFS and GS. LOI values for all 3 samples were negative, which could be explained by Fe oxidation during sample sintering (Vandenberghe et al., 2010).

In case of minor elements, LS sample is the most abundant in Cu, Pb and Zn (0.74, 0.89 and 4.6 wt%, respectively). The reason behind this is the fact that LS sample is derived from the lead recovery process in Dörschl reverberatory furnace, where the feed is rich in metals (e.g. Pb, Cu, Zn) not recovered in other parts of the process. Among minor elements, very abundant are metals that are potentially attractive from resource perspective. All three slags (LS, SFS and GS) are enriched in Co (187, 1446 and 627 mg kg^{-1}, respectively), Mo (164, 773 and 296 mg kg^{-1}, respectively) and V (598, 1228 and 1168 mg kg^{-1}, respectively) compared to crustal average values of these elements (Taylor, 1964). Rare earth elements (REE) are abundant in slags as well (94, 255 and 308 mg kg^{-1} for LS, SFS and GS, respectively). The LS and SFS slags contain some amounts of Au (3200 and 1600 ppb, respectively). The patterns of REE shown on Fig. 1 indicate an enrichment in LREE compared to HREE for all samples, especially when normalized against chondritic meteorites, where the enrichment factor is equal to ca. 300 for La and ca. 200 for Ce (Fig. 1C). After normalization against North American shale composite (Fig. 1A) patterns for all samples show negative Eu and Tb anomalies and positive Gd anomaly, which is most visible for the SFS and LS, although REE content in LS is the lowest (enrichment factors < 1). The negative Eu anomaly is also visible after normalization against chondrites (Fig. 1C), again for SFS and LS. The reasons for negative europium anomaly are connected with changing oxidation state of Eu from +3 to +2 and substitution for Ca^{2+} in other minerals that crystallized first (Bau, 1991). On the other hand, REE pattern for GS after normalization against the upper continental crust (Fig. 1B) shows a small positive Eu anomaly. This might be derived from accumulating crystals before solidification, which is apparent in case of GS as amorphous material.

Table 2
Chemical composition of the studied slags (LS - lead slag, SFS - shaft furnace slag, GS - granulated slag).

Chemical components [wt%]	Major elements			Chemical components [ppm]	Minor elements			Chemical components [ppm]	Rare earth elements		
	LS	SFS	GS		LS	SFS	GS		LS	SFS	GS
SiO_2	33.05	43.72	38.27	Cu	7415	2795	7067	Y	13.0	30.2	38.8
Al_2O_3	5.73	12.45	12.39	Pb	8959	2950	7990	La	22.4	60.8	77.6
Fe_2O_3*	33.42	18.91	11.53	Zn	46020	15407	5046	Ce	36.5	110	129
MgO	4.99	6.48	6.33	Ni	77.4	90.3	110	Pr	4.57	11.5	13.5
CaO	10.37	11.57	23.56	As	273	44.8	170	Nd	17.9	41.2	49.7
Na_2O	3.43	0.80	0.98	Cd	44.4	0.80	2.60	Sm	2.95	7.57	9.69
K_2O	2.87	3.45	3.43	Sb	5.70	1.90	0.40	Eu	0.63	1.69	2.57
TiO_2	0.30	0.66	0.69	Sn	232	78.0	7.00	Gd	2.98	7.38	8.62
P_2O_5	0.13	0.20	0.14	Bi	10.3	≤0.01	0.20	Tb	0.38	1.03	1.26
MnO	0.48	0.26	0.28	Ag	8.90	6.70	1.80	Dy	2.51	5.64	7.00
Cr_2O_3	0.58	0.18	0.05	Au [ppb]	3200	1600	≤0.5	Ho	0.49	1.07	1.43
S total	2.67	0.21	0.05	Co	187	1446	627	Er	1.31	3.01	3.80
LOI	−3.50	−2.00	−1.10	Mo	164	773	296	Tm	0.18	0.39	0.51
* - total Fe				V	598	1228	1168	Yb	1.02	2.46	2.92
				W	19.9	19.7	3.70	Lu	0.17	0.38	0.42
				Sr	205	361	487	ΣREE	94.0	255	308
				Rb	134	140	148	ΣREE + Y	107	285	347

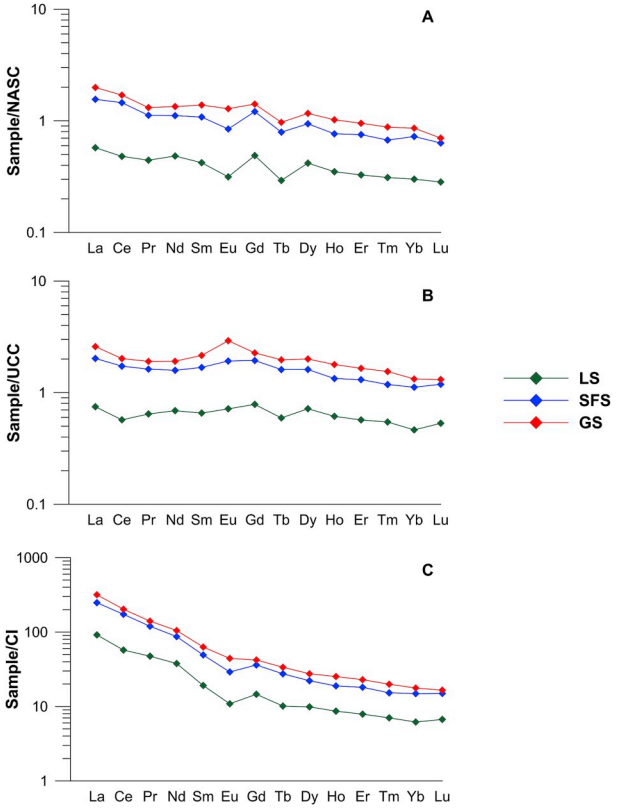

Fig. 1. REE patterns of lead slag (LS), shaft furnace slag (SFS) and granulated slag (GS) normalized against: A) North American shale composite (NASC; after Gromet et al., 1984), B) upper continental crust (UCC; after Taylor and McLennan, 1985) and C) meteoritic chondrites (CI; after Evensen et al., 1978).

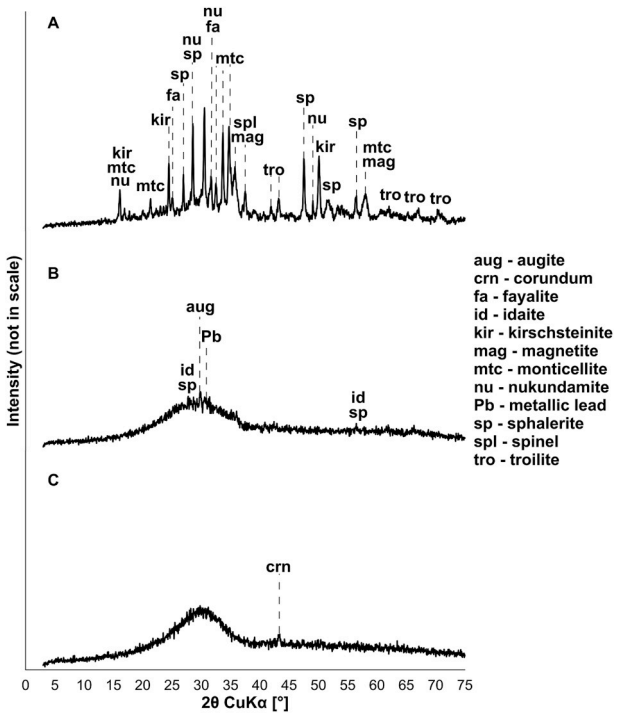

Fig. 2. X-Ray diffraction patterns of lead slag (A), shaft furnace slag (B) and granulated slag (C).

4.2. Mineralogy

In this paper, phase components are referred to natural equivalents of minerals. The reason for that is the difference in "mineral" definition in pure and applied mineralogy. This time, authors followed the definition proposed by A.N. Winchell and H. Winchell (1964) and Szymański (1989), who stated that minerals are not only geologically formed phases, but also the constituents of synthetic materials and metallurgical residues. Mineral abbreviations used in Figs. 3–7 (except for Cu sulfides) are after Whitney and Evans (2010).

4.2.1. Slag petrography

The studied slags demonstrate distinctly different mineralogical compositions. In all samples, the silicate glass is the main constituent, as expressed on XRD patterns (Fig. 2). LS slag is composed of glassy matrix, but in this material the number of crystalline phases is substantial (Fig. 2A). Among crystallites, silicates (such as olivines) and sulphides (e.g. bornite, sphalerite, pyrrhotite) are most abundant. Some metallic inclusions (Cu, Pb, Fe) and spinel oxides were also determined in the LS sample. In case of SFS and GS, the metal silicate glass is virtually sole component (Fig. 2B and C), along with metallic inclusions (Cu, Pb, Co-Ni-Fe-Cu-As alloy) and some sulphides (bornite, sphalerite) present in SFS sample.

Lead slag (LS). Microscopic study shows that olivine forms euhedral crystals from several to 250 µm (Fig. 3A-C). The olivine crystals are either of regular (Fig. 3A and C), elongated (Fig. 3B) or needle-like (Fig. 3A) shape. Oxides represented by spinels are either found as inclusion in olivine (Fig. 3A) or form euhedral, isometric crystals (circular, orthogonal or hexagonal) but irregular grains are also common (Fig. 3A). Their size is up to 20 µm in diameter. Crystals display zonation (Fig. 3A and B), sometimes accompanied by magnetite rims (Fig. 3B and D). Magnetite was also found as dendrites in the vicinity of bigger zoned spinel crystals (Fig. 3D). Sulfides are either found as droplets in silicate matrix (Fig. 3A–C) or as solitary grains of up to 1 mm in size (Fig. 4). The sulfide grains were found to be formed by bornite with intergrowths of pyrrhotite (Fig. 4A, B1, 4E, 4F) or as pyrrhotite-sphalerite mixtures (Fig. 4C). Sphalerite was found as solitary grains (up to 100 µm) encapsulated in bigger sulfide aggregates (Fig. 4A, B1, 4E). Metallic aggregates, consisting of Cu and Pb spherules, are commonly found in sulfide grains (Fig. 4A–D). The assemblage of pyrrhotite and löllingite was also observed near Pb metallic grains (Fig. 4B2). Metallic Fe is present as droplet inclusions within sphalerite (Fig. 4D) and are accompanied by metallic Pb inclusions.

Shaft furnace slag (SFS) and granulated slag (GS). Both the SFS and GS samples were found to be composed mainly of glassy silicate solid solution. In case of SFS, sulfides were found as solitary grains up to 120 µm in the studied sample (Fig. 5A and C) or as spherule inclusions in glass (Fig. 5B and D). Sulfide grains, composed of bornite, are accompanied by intergrowths of sphalerite and tiny metallic inclusions of Co-Ni-Fe-Cu-As alloy and metallic Pb (Fig. 5A-C). Metallic Cu was found as tiny intergrowths within bornite-sphalerite spherules (Fig. 5D1). Bornite spherules are also accompanied by Co-Ni-Fe-Cu-As alloy (Fig. 5D2). Spinels in GS occur as ca. 200-µm inclusions in glassy matrix and are not zoned (Fig. 5E and F). Metallic Cu was also found in the form of droplets within spinels (Fig. 5E). The Cu-Pb droplets in GS sample are the only crystalline phases found within the glass matrix (Fig. 6). The metallic droplets (up to 15 µm in size) are composed of metallic Cu with metallic Pb intergrowths (Fig. 6B2).

4.2.2. Chemistry of phases

4.2.2.1. Glassy matrix. The glass silicate phase was observed in all three examined materials. The chemical composition of the glass matrix (Table 3) is slightly different in each slag. The glass is rich in Fe, Al and Ca. The content of Fe and Al is similar for each material; however, GS is most rich in Ca (up to 30 wt% CaO, 24 wt% average). Glass from all studied slag samples is rich in Zn, mostly in LS (up to 8.75 wt% ZnO). Cu is present in glass from both SFS and GS (up to 3.38 wt% CuO,

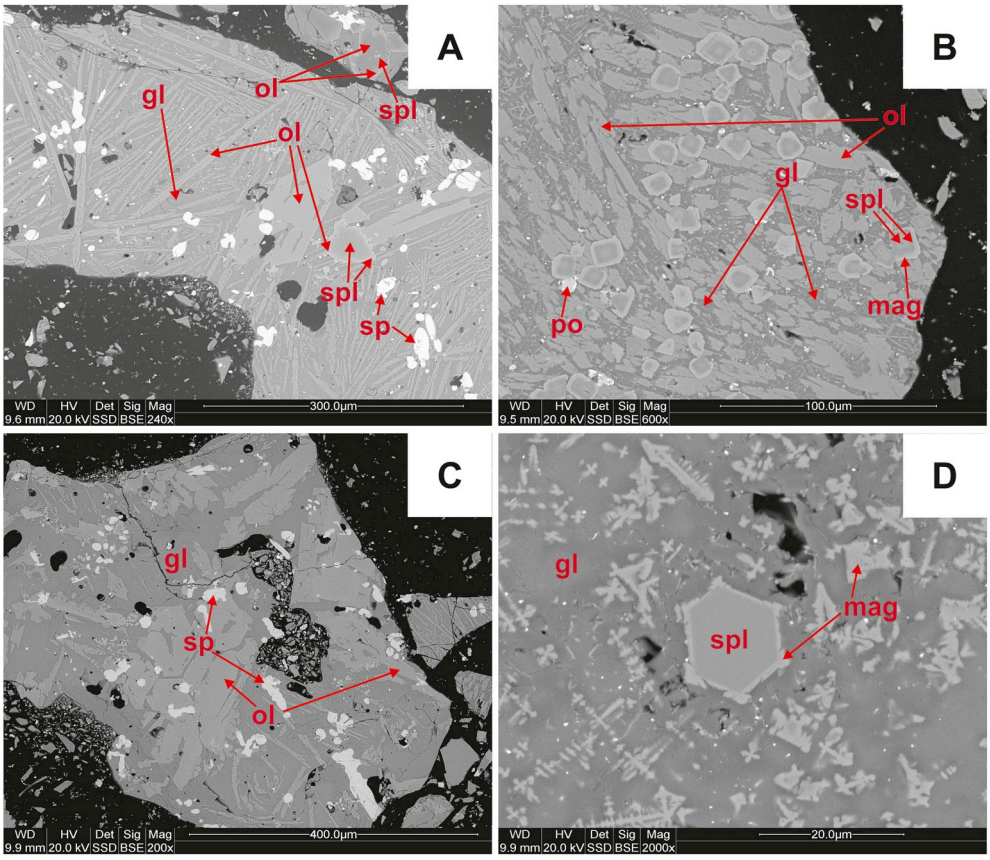

Fig. 3. BSE photomicrographs of LS sample showing glass matrix (gl) enclosing silicates and oxides; A) euhedral olivine (ol), spinel (spl) grain with olivine rim and sphalerite (sp) inclusions; B) glass matrix (gl) with elongated euhedral olivine (ol) crystallites, spinel (spl) zoned grains with magnetite (mag) rims and tiny pyrrhotite (po) inclusions; C) euhedral olivine (ol) crystals and sphalerite (sp) inclusions in glass matrix (gl); D) hexagonal spinel (spl) zoned grains with magnetite (mag) rims and magnetite dendritic crystallites in the glass matrix (gl).

2.33 wt% average).

4.2.2.2. Silicates. Crystalline silicate phases occur only in LS, forming euhedral crystals of various shapes (Fig. 3A-C). Chemically, these phases are close to olivine (Table 4). Three different types of olivine were recognized in terms of chemical composition, two of them presumably being members of forsterite (Mg_2SiO_4) - fayalite (Fe_2SiO_4) solid solution (Olivine 1 and Olivine 2). Olivines 1 and 2 form regularly shaped or needle crystals (Fig. 3A and C). Olivine 3, which forms elongated crystals (Fig. 3B), is rich in Ca (up to 20.65 wt% CaO); chemical composition suggests that it is a member of monticellite ($CaMgSiO_4$) - kirschsteinite ($CaFe^{2+}SiO_4$) solid solution. All types of olivine are non-stoichiometric, with 1.63–1.79 atoms per formula unit of divalent cations. This phenomenon is probably linked to the presence of Al, K and Na, coming from the glass matrix, in olivine phases (Table 4). Olivine phases contain zinc (up to 5.14 wt% ZnO), which probably is substituted for Fe in octahedral site of the phase (Ettler et al., 2009).

4.2.2.3. Spinel oxides. Oxide phases in the form of spinel oxides are present only in LS (Fig. 3A, B, 3D) and SFS (Fig. 5E and F). In general, spinel oxides in both types of slag are deviated from pure spinel formulas and were probably formed from different solid solutions (Table 5).

Lead slag (LS). Four different types of spinels can be distinguished in LS. Spinels 1 and 2 are present as zoned euhedral crystals of irregular shape (Fig. 3A). The inner core of these crystals (Spinel 1) is rich in Mg (up to 22.8 wt% MgO) and poor in Zn, as is opposite to the outer part (Spinel 2), which has up to 12 wt% of ZnO. Spinel 2 is also found in droplet inclusions in olivine (Fig. 3A). Spinels 3 and 4 are present as zoned, euhedral, regular-shaped crystals (Fig. 3B and D). Inner core of these crystals (Spinel 3) is enriched in Cr compared to outer core (Spinel 4), which is rich in Al instead of Cr and contains higher amount of Fe^{3+} (Table 5). Spinel 1 contains some amount of Co (up to 0.39 wt% Co_2O_3). Spinels 2–4 are rich in V (up to 1.59 wt% V_2O_3). All types of spinels are rich in Zn (up to 3.20 wt% ZnO, except of Spinel 2). Presumably, these phases represent solid solutions between phases such as zincochromite ($ZnCr_2O_4$), magnesiochromite ($MgCr_2O_4$), franklinite ($ZnFe_2O_4$), magnesioferrite ($MgFe_2O_4$), spinel ($MgAl_2O_4$) and hercynite ($FeAl_2O_4$). The rims of zoned spinel crystals appear as magnetite (Magnetite 1) as shown by microscopic observations (Fig. 3B and D). The other type of "magnetite" (Magnetite 2) forms dendritic crystals in glass matrix (Fig. 3D). Magnetite 1 and 2 are composed mainly of Fe^{2+} and Fe^{3+}, but considerable amounts of Al (higher in Magnetite 1; up to 18.73 wt% Al_2O_3) were determined in these phases; chemical composition suggests that the crystals represent magnetite ($Fe^{2+}Fe_2^{3+}O_4$) - hercynite ($FeAl_2O_4$) solid solution. Magnetite 1 contains also some amount of V (up to 1.13 wt% V_2O_3). Last type of magnetite (Magnetite 3) is found in mineral assemblages containing sulphides (Fig. 4F), and probably for this reason it is enriched in Cu (up to 3.17 wt% CuO) and impoverished in Al compared to other types. All magnetites are rich in Zn (up to 3.39 wt% ZnO).

Shaft furnace slag (SFS). Two types of spinel oxides were found in SFS. First type (Spinel 1) forms inclusions in glass matrix that are intergrown with Cu droplets. This is probably the reason for elevated Cu content in this phase (up to 26 wt% CuO; 2.99 wt% in average). Spinel 1 is composed mainly of Mg, Cr and Al, which suggests that this phase represents magnesiochromite ($MgCr_2O_4$) - spinel ($MgAl_2O_4$) solid solution. It also contains some amounts of Zn, Ni and Co (Table 5). Second type of spinel (Spinel 2) also forms inclusions in glass (Fig. 5F). Spinel 2 is poor in Mg and Al, but rich in Fe^{2+}, suggesting that the phase represents chromite ($FeCr_2O_4$) - magnesiochromite ($MgCr_2O_4$) solid solution.

4.2.2.4. Sulfides. Sulfides occur in LS and SFS samples in the form of bornite (Cu_5FeS_4), sphalerite (ZnS) and (only in LS) pyrrhotite (Fe_7S_8). Chemical compositions of sulfides are shown in Table 6.

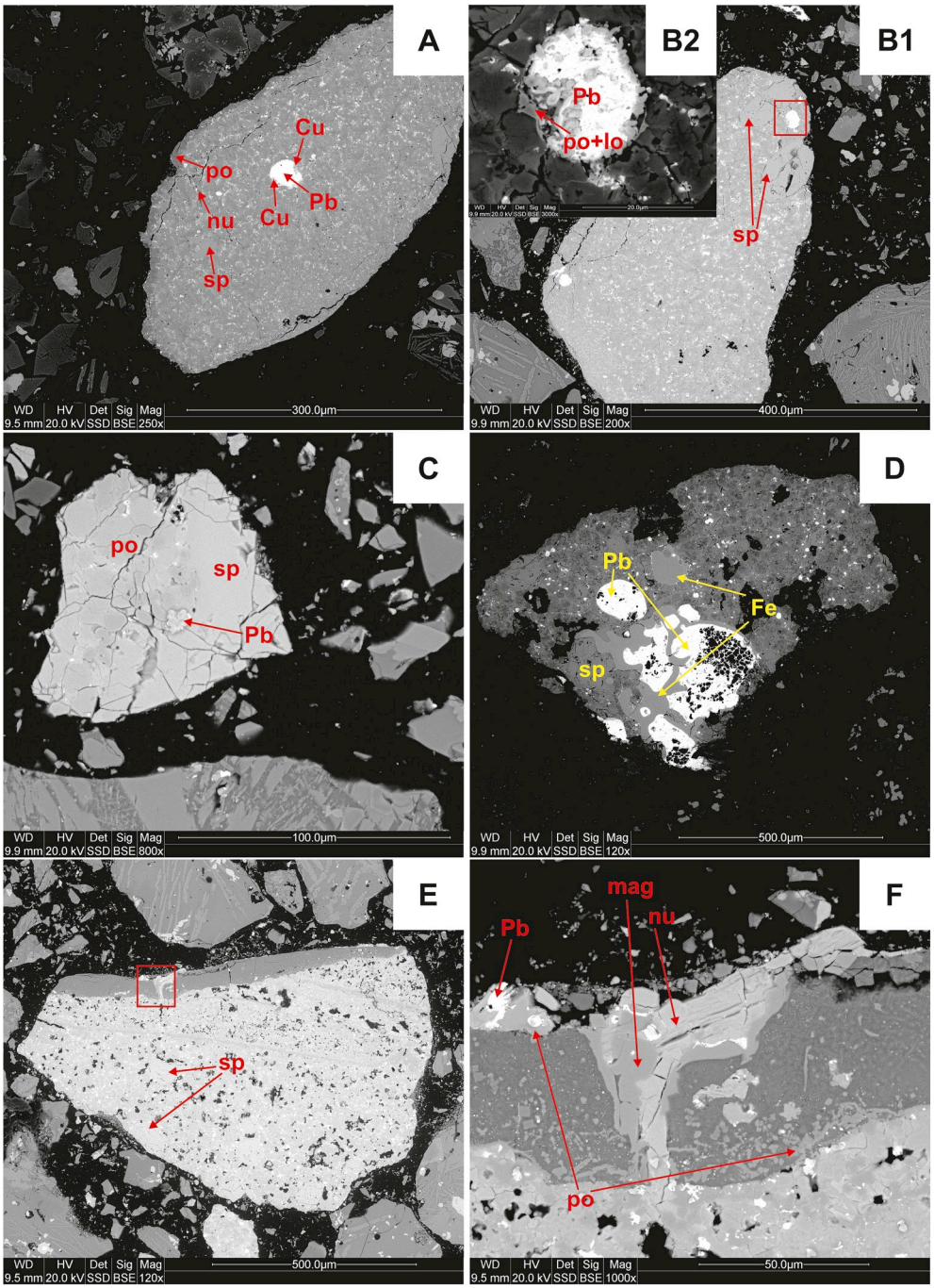

Fig. 4. BSE photomicrographs of LS sample showing sulfides and intermetallic compounds; A), B1) nukundamite (nu) grains with pyrrhotite (po) and sphalerite (sp) intergrowths and with Cu and Pb metallic inclusions; B2) magnification of red rectangle from B1, showing Pb metallic spherule with pyrrhotite-löllingite grain (po + lo); C) pyrrhotite (po)-sphalerite (sp) grain with metallic Pb inclusion; D) sphalerite (sp) grain with metallic Pb and Fe droplets; E) nukundamite (nu) grain with pyrrhotite (po) and metallic Pb intergrowths and sphalerite (sp) grains; F) magnification of red rectangle from E; showing nukundamite-pyrrhotite-magnetite-Pb assemblage. (For interpretation of the references to colour in this figure legend, the reader is referred to the Web version of this article.)

Copper-iron sulfides in both LS and SFS resemble bornite when observed under optical microscope. However, "bornite" from LS is more similar to nukundamite [$(Cu, Fe)_4S_4$], but rich in Fe (up to 24 wt%). Similarity complex composition was also revealed on XRD pattern (Fig. 2A), where strongest peaks of nukundamite occur together with sphalerite. On the other hand, "bornite" from SFS is chemically more similar to idaite (Cu_3FeS_4), although impoverished in S and slightly enriched in Fe compared to pure idaite composition. The phases in question are the secondary products of bornite and chalcopyrite ($CuFeS_2$) alteration processes (Rice et al., 1979), but in case of slag melt they probably were formed from solid solution of these primary phases. The nukundamite from LS contains some Zn (up to 1.5 wt%). Both nukundamite and idaite are rich in As (up to 2.79 wt%), Sn (up to 0.56 wt%), Sb (up to 0.23 wt%) and Co (up to 0.4 wt%) (data not shown).

Two different types of Fe-bearing sphalerites can be distinguished in LS sample (Table 6). The first type (Sphalerite 1) is less rich in Fe (up to 14 wt%) and was found as intergrowth in sulfidic grains (Fig. 4A, B1). The second, Cu-bearing (up to 2.5 wt%) type (Sphalerite 2) is more rich in Fe (up to 23 wt%). It was found in solitary ZnS grains encompassed by bigger sulfidic grains (Fig. 4A, B1, 4D) or as co-forming phase of pyrrhotite-sphalerite grains (Fig. 4C). Sphalerite from SFS is also Fe-bearing (up to 25 wt%) and rich in Cu (up to 6.5 wt%). The occurrences of As (up to 0.72 wt%) and Cd (up to 0.21 wt%) were also found in sphalerite from SFS sample.

Pyrrhotite was found solely in LS sample. Although microscopic observations revealed that this phase resembles pyrrhotite, XRD analysis (Fig. 2) suggests that it has structural features of troilite (FeS). Iron sulfide from LS can be divided into two types (Table 6). First type (Pyrrhotite 1) is extremely rich in Cu (up to 18.5 wt%) and was found as component of sulfidic grains (Fig. 4A and F); another component of

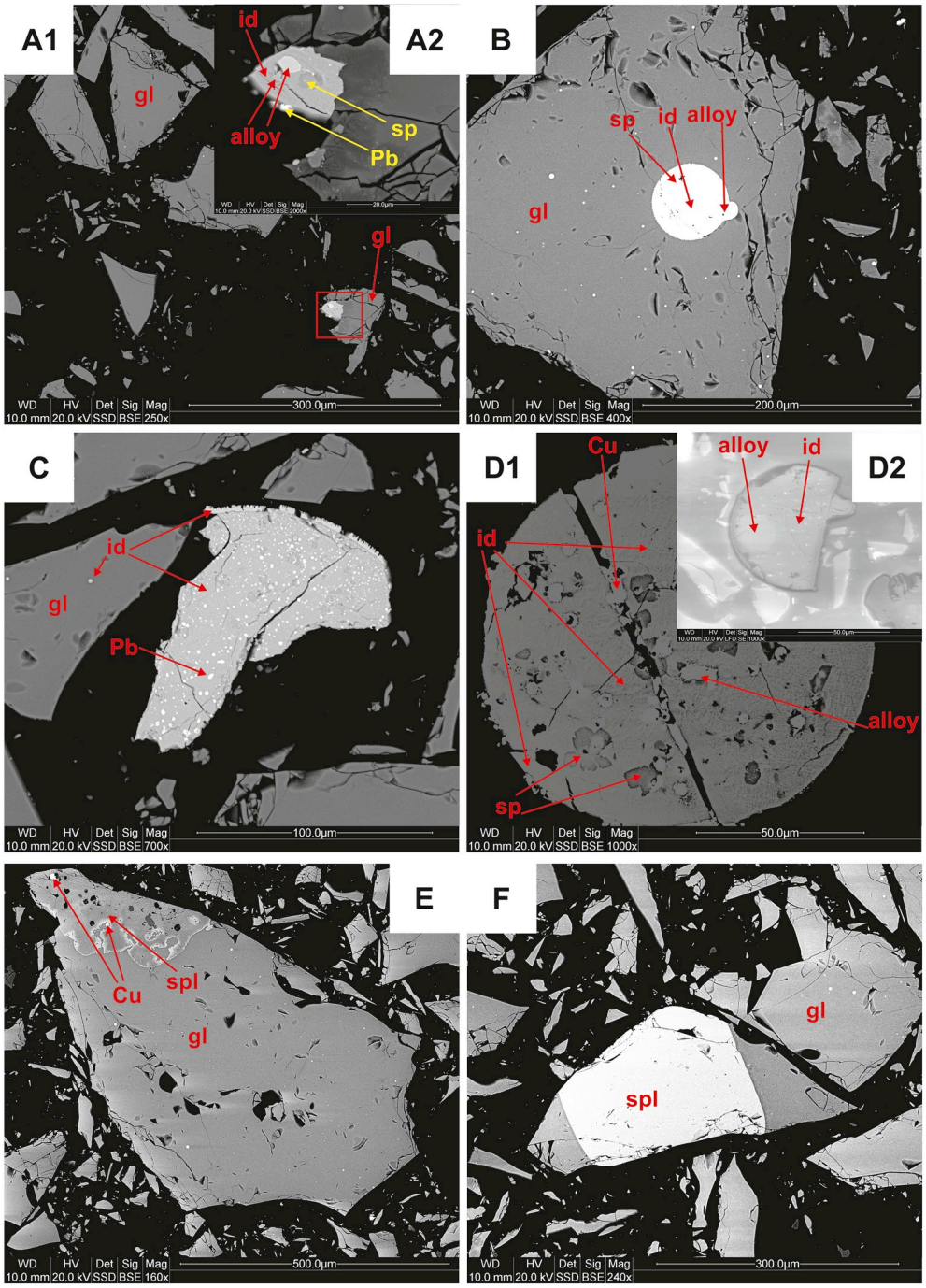

Fig. 5. BSE photomicrographs of SFS sample; A1) glass matrix (gl) with small sulfide grains; A2) magnification of red rectangle from A1, showing idaite (id) grain with sphalerite inclusion (sp), Co-Ni-Fe-Cu-As alloy and metallic Pb inclusions; B) glass matrix (gl) with droplets consisting of idaite (id), sphalerite (sp) and Co-Ni-Fe-Cu-As alloy; C) idaite (id) grain with fine metallic Pb droplets and glass matrix fragment (gl) with solitary idaite (id) inclusions; D1) idaite sphere (id) with inclusions of sphalerite (sp) metallic Cu and Co-Ni-Fe-Cu-As alloy; D2) insertion of magnified secondary electron (SE) image of one of idaite (id) droplets with inclusion of Co-Ni-Fe-Cu-As alloy; E) spinel (spl) and metallic Cu inclusions in glass matrix (gl); F) spinel (spl) inclusion in glass matrix (gl). (For interpretation of the references to colour in this figure legend, the reader is referred to the Web version of this article.)

these grains is nukundamite, hence the bigger Cu enrichment. Second type (Pyrrhotite 2) is less abundant in Cu (up to 1.5 wt%). It was found as co-component of pyrrhotite-sphalerite grains (Fig. 4C) and in pyrrhotite-löllingite association (Fig. 4B2), where As replaced S and its content reaches 9.3 wt%. Both types are contaminated by Zn (up to 2.5 wt%); also, Sn (up to 1.28 wt%), Sb (up to 0.33 wt%) and Ni (up to 1.45 wt%) (data not shown).

4.2.2.5. Intermetallic compounds. Various intermetallic compounds, including Pb, Cu, Fe and polymetallic alloys were found in all three examined slags in the form of droplets or droplet-like inclusions. Metallic Pb and metallic Cu are present in all examined materials and their composition varies in different slags (Table 7).

Metallic Cu from LS contains less Cu (up to 72.87 wt%); but it is a major carrier of Fe (up to 7 wt%), Sn (up to 5.33 wt%) and Sb (up to 2.31 wt%), Ni (up to 0.81 wt%), Te (up to 0.71 wt%) and Co (up to 0.34%) (data not shown). In case of SFS and GS, Cu content in metallic Cu is much higher (up to 98.64 wt%). Metallic Cu from SFS is contaminated by Cr (up to 6.83 wt%) and As (up to 1.17 wt%); on the other hand, metallic Cu from GS is a major As carrier (up to 10.38 wt%). Admixtures of Ni (up to 0.86 wt%) and Co (up to 0.54 wt%) were also determined (data not shown).

Inclusions of metallic Pb are fairly pure (up to 95.4 wt% Pb) in all examined slags. In the case of LS sample, Fe (up to 10.72 wt%) and Zn (up to 6.56 wt%) are the main contaminants in Pb inclusions; some Te (up to 0.56 wt%), Co (up to 0.76 wt%) and Sn (up to 1.82 wt%) are also present (data not shown). Pb inclusions from SFS and GS samples are rich in Cu (up to 13.17 wt%) and Fe (up to 6.09 wt% in SFS and 1.06 wt % in GS) with occurrences of Zn and As (Table 7).

Metallic Fe droplets occur solely in LS sample. The Fe content

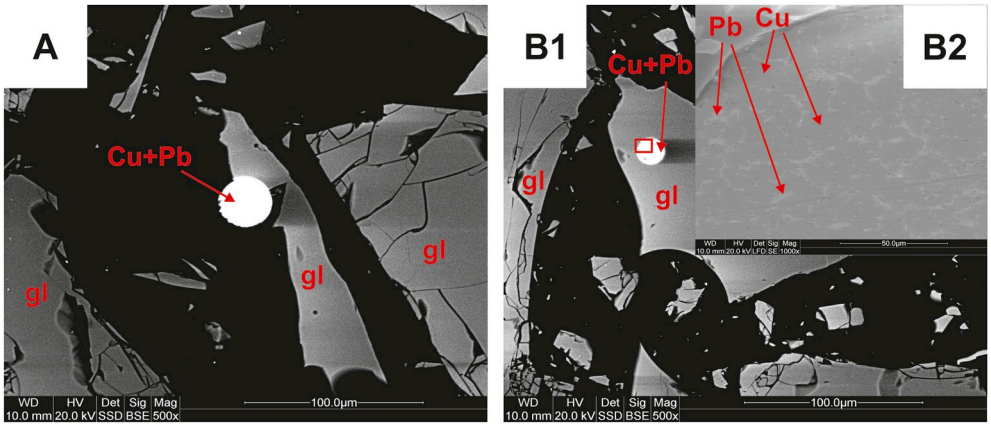

Fig. 6. BSE photomicrographs of GS sample; A), B1) metallic Cu-Pb inclusions in glass matrix (gl); B2) secondary electron (SE) magnification of red rectangle from B1 showing the structure of Cu metallic inclusion with Pb intergrowths. (For interpretation of the references to colour in this figure legend, the reader is referred to the Web version of this article.)

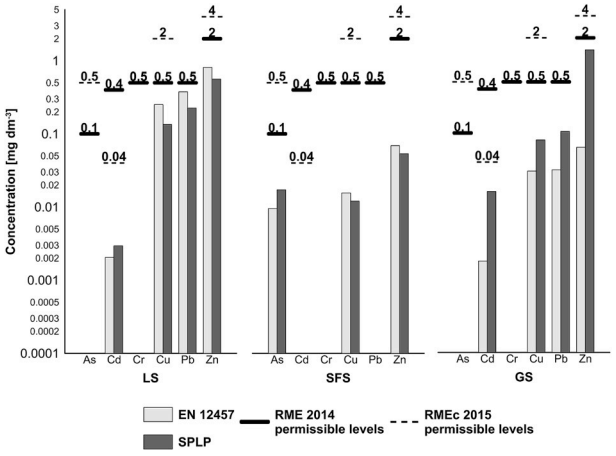

Fig. 7. Comparison of SPLP and EN12457 leaching tests results for lead slag (LS), shaft furnace slag (SFS) and granulated slag (GS) compared with limits for selected elements according to the Polish legal acts concerning permissible levels of metal concentrations in wastewaters (RME, 2014) and leachates for non-hazardous wastes (RMEc, 2015).

reaches 92.70 wt%. The main contaminant is As (up to 9.69 wt%), suggesting the admixture of metallic As or löllingite. Inclusions of Fe contain metals such as Cu and Sn (up to 2.11 and 0.4 wt%, respectively; Table 7), as well as Zn, Ni and La (up to 1.19, 0.99 and 1.11 wt%, respectively; data not shown).

Another polymetallic compound, found only in SFS sample, is a polymetallic alloy, which can be generally referred to as Co-Ni-Fe-Cu-As alloy (Table 7). Various concentrations of these five elements were measured, but in average, this phase is the main Co, Ni and As carrier in SFS (up to 46.76, 37.92 and 25.34 wt%, respectively). Occurrences of metals such as Sb (up to 6.68 wt%; Table 7), Sn (up to 1.76 wt%), Te (up to 0.31 wt%), Bi (up to 2.16 wt%), Au (up to 0.67 wt%) and Se (up to 1.48 wt%) were determined in the alloy (data not shown).

4.3. Mobility of metals

4.3.1. Leaching with water and simulated rainfall

The results of leaching tests and comparison to regulatory levels are shown on Fig. 7. Values of leached metal(loid)s are reported in Table 8. Elements such as As and Cr were below detection limits, except for SFS, where leaching of As (up to 0.017 mg dm^{-3}) took place. Metals such as Cd and Pb were also not reported in leachates from SFS sample. The highest values of leaching for Cu and Pb were reported for SPLP test in LS sample (0.135 and 0.225 mg dm^{-3}, respectively), and for Zn in GS sample (1.366 mg dm^{-3}). Values of metal(loid)s leached by distilled water were similar to those obtained by simulated rainfall (except for Zn - 0.064 mg dm^{-3}), although initial pH was different (6.5 for water and 4.2 for rain medium). The similar final pH values (7.3–8.5 for precipitation, 8.5–9.3 for water) confirm that the values should be comparable and even higher for rain medium, but in case of Cu, Pb and Zn for SFS and LS samples the values of water leaching (up to 0.251, 0.377 and 0.810 mg dm^{-3}, respectively) were slightly higher than for simulated precipitation (up to 0.135 mg dm^{-3} Cu, 0.225 mg dm^{-3} Pb and 0.560 mg dm^{-3} Zn).

4.3.2. Sequential extraction

The six-step sequential extraction revealed the geochemical forms in

Table 3
Composition of glass matrix determined in lead slag (LS), shaft furnace slag (SFS) and granulated slag (GS).

Chemical components [wt%]	Glass								
	LS (n = 4)			SFS (n = 9)			GS (n = 5)		
	Max	Min	Average	Max	Min	Average	Max	Min	Average
SiO_2	50.97	42.11	48.04	50.84	40.87	45.51	47.33	43.56	44.72
Al_2O_3	22.83	6.80	12.53	20.09	12.83	15.63	15.46	13.34	14.75
FeO	23.44	13.86	18.73	18.29	11.86	16.18	13.56	8.93	10.52
MgO	4.73	0.98	1.94	9.70	5.39	6.95	7.45	4.59	6.72
CaO	13.59	6.83	8.92	12.79	8.47	9.98	30.24	21.77	23.91
Na_2O	5.04	0.00	2.16	2.24	0.82	1.82	1.75	1.00	1.50
K_2O	7.31	4.61	5.98	3.47	2.46	3.06	5.46	3.60	4.05
CuO	na	na	na	2.54	0.00	0.69	3.38	1.23	2.33
ZnO	8.75	1.48	4.98	2.14	0.00	1.71	1.41	0.00	0.87
TiO_2	0.48	0.00	0.32	0.85	0.53	0.70	1.15	0.60	0.80
MnO	0.68	0.00	0.17	0.43	0.00	0.08	0.65	0.00	0.16

na - not analyzed.

Table 4
Composition of olivines determined in lead slag (LS).

Chemical components	LS	LS	LS
	Olivine 1	Olivine 2	Olivine 3
SiO_2 *wt%*	39.78	37.14	37.40
Al_2O_3	1.08	1.34	2.10
FeO	19.73	39.59	32.73
MgO	34.24	14.84	6.95
CaO	2.73	2.83	20.64
ZnO	3.82	5.14	1.32
Na_2O	3.53	na	1.05
K_2O	0.47	0.51	0.71
MnO	0.74	1.06	0.75
Si *apfu*	0.96	1.04	1.02
Al	0.06	0.09	0.13
Fe	0.40	0.93	0.75
Mg	1.23	0.62	0.28
Ca	0.07	0.08	0.60
Zn	0.07	0.11	0.03
Na	0.08	0.00	0.03
K	0.01	0.01	0.01
Mn	0.02	0.03	0.02

na - not analyzed.

which selected elements occur in the slags (Fig. 8). This varies depending on type of slag. Some metals were totally leached from slags (Cu, Pb) and some of them were only partly leached, again depending on the type of examined material. The leached metals are expressed as fraction of total concentration of elements [%] (Table 2).

Metal(loid)s from LS sample display different leaching behavior, except for Cd and Cu, that again are mostly (92% and 73%, respectively) bound to sulfides and residual fraction (F5-F6). Contrary to SFS, elements such as As and Pb are mostly bound to F1-F4 fractions (40% and 59%, respectively). The results of Zn leaching show that F1-F4 fractions contain 37% of Zn in LS and 47% of Zn in SFS. These findings correspond to substantial amounts of Zn in LS (ca 17000 mg kg^{-1}) and in SFS (7250 mg kg^{-1}) that can be released into the leachate and pose threat to nearby environments. 38% of Zn is bound to F5 (sulfides), which corresponds to high content of ZnS in LS sample. The amount of Cr leached from LS sample is 4.4%, mostly (2.5%) in residual fraction (F6).

In the case of SFS, elements such as As, Cd, Cu and Pb are carried mainly by sulfides and residual fraction (F5 and F6). However, 20% of Pb is bound to ion exchangeable, carbonate and Fe-Mn oxide fractions (F1-F4). On the other hand, metals such as Cr and Zn are mostly (80% Cr and 47% Zn, respectively) bound to F1-F4 fractions. This finding, combined with total concentrations of Cr, Pb and Zn shows that considerable amounts of metals can be leached out (1416, 590 and 7241 mg kg^{-1}, respectively). The low concentration of Zn in the sulfide (F5) fraction (3.2%) shows that sulfides as main carriers of Zn (sphalerite) do not release Zn into this solution. Contrary, high Cr content (54.5%) in the Fe-oxide fraction (F3-F4) shows that either main carriers of Cr (spinel oxides) are susceptible to leaching, probably due to their occurrence as inclusions in glass matrix, or the glass matrix itself contains high amount of Cr. This was confirmed by high Fe release in this step (41%, data not shown), which is abundant both in spinels and glass matrix. To examine the leaching potential of silicate glass and spinel oxides, one drop (ca. 0.1 cm^3) of citrate buffer used to dissolve F4 fraction (see Table 1) was placed onto the spinel/glass assemblage present in the SFS sample. The liquid was in contact with the slag for 20 min and subsequently observed with reflected light microscope. The experiment revealed that spinel oxides were not dissolved by citrate buffer. On the other hand, the glass silicate phase has been dissolved partially within 20 min. The resistance of spinel oxides to dissolution has been previously reported in the literature (e.g. Bril et al., 2008).

Leaching results of GS sample show that all elements (except for As and Cd) were completely leached out. The leached amount of Cd is 40%, 25% being in mobile forms (F1-F4), which corresponds to 0.65 mg kg^{-1} leached out, which does not pose any notable threat. The examined metal(loid)s have their mobile content as follows: As 62%, Cr 66%, Cu 61%, Pb 64% and Zn 69%. The mentioned values correspond to substantial amounts of these elements (As - 105 mg kg^{-1}, Cr - 319 mg kg^{-1}, Cu - 4311 mg kg^{-1}, Pb - 5138 mg kg^{-1}, Zn - 3482 mg kg^{-1}) that could be released to the environment.

Table 5
Composition of investigated spinel oxides determined in lead slag (LS) and shaft furnace slag (SFS).

Chemical components	LS	LS	LS	LS	LS	LS	LS	SFS	SFS
	Spinel 1	Spinel 2	Spinel 3	Spinel 4	Magnetite 1	Magnetite 2	Magnetite 3	Spinel 1	Spinel 2
Al_2O_3 *wt%*	14.36	11.51	19.16	41.08	18.73	11.03	2.02	25.28	17.54
Fe_2O_3	7.62	30.23	24.00	39.00	54.00	65.28	79.02	5.49	6.44
FeO	na	na	4.76	5.48	15.08	7.26	10.40	na	18.98
MgO	22.80	5.70	7.91	9.35	2.50	4.44	0.95	20.79	9.63
Cr_2O_3	49.34	33.54	35.65	0.61	na	2.56	na	41.32	43.51
CuO	na	na	0.68	na	na	na	3.27	2.99	na
ZnO	1.74	11.96	3.20	3.14	3.39	2.89	3.17	1.13	na
NiO	na	na	na	na	na	na	na	0.79	na
TiO_2	na	0.48	0.62	1.87	4.57	0.63	na	na	0.68
MnO	na	na	na	0.59	0.59	0.90	na	na	0.56
V_2O_3	na	0.34	0.72	1.59	1.13	na	na	na	na
Co_2O_3	0.39	na	na	na	na	na	na	0.75	na
Al *apfu*	0.55	0.43	0.65	1.22	0.69	0.41	0.08	0.89	0.69
Fe^{3+}	0.19	0.72	0.52	0.74	1.28	1.53	1.92	0.12	0.16
Fe^{2+}	0.00	0.00	0.17	0.09	0.36	0.38	0.58	0.00	0.49
Mg	0.96	0.48	0.65	0.70	0.23	0.41	0.09	0.89	0.48
Cr	1.26	0.84	0.81	0.01	0.00	0.06	0.00	0.97	1.15
Cu	0.00	0.00	0.03	0.00	0.00	0.00	0.17	0.07	0.00
Zn	0.04	0.50	0.13	0.12	0.16	0.13	0.16	0.02	0.00
Ni	0.00	0.00	0.00	0.00	0.00	0.00	0.00	0.02	0.00
Ti	0.00	0.02	0.03	0.07	0.22	0.03	0.00	0.00	0.02
Mn	0.00	0.00	0.00	0.03	0.03	0.05	0.00	0.00	0.02
V	0.00	0.01	0.02	0.03	0.03	0.00	0.00	0.00	0.00
Co	0.01	0.00	0.00	0.00	0.00	0.00	0.00	0.02	0.00

na - not assigned.

Table 6
Composition of investigated sulfides determined in lead slag (LS) and shaft furnace slag (SFS).

Chemical components	LS	LS	LS	LS	LS	SFS	SFS
	Nukundamite	Sphalerite 1	Sphalerite 2	Pyrrhotite 1	Pyrrhotite 2	Idaite	Sphalerite
S *wt%*	32.81	33.14	35.33	36.10	37.28	27.39	34.31
Fe	23.77	13.96	22.39	42.82	59.02	16.72	24.46
Cu	42.01	na	2.22	18.45	1.37	55.89	6.24
Zn	1.41	52.89	40.06	2.14	2.33	na	31.27
S *apfu*	4.00	1.00	1.00	8.00	8.00	4.00	1.00
Fe	1.54	0.24	0.38	4.92	6.64	1.00	0.41
Cu	2.39	0.00	0.03	1.86	0.14	3.00	0.09
Zn	0.08	0.76	0.58	0.21	0.22	0.00	0.48

na - not assigned.

5. Discussion

5.1. Mineralogical and chemical composition

Results of mineralogical investigation of copper smelting by-products is reflecting different characteristics of the processes that led to generation of these slags. Parameters such as cooling regime and furnace feeds seem to play a major role in composition differences. Studied materials consist mainly of glass and do not contain clinopyroxene crystallites that are believed to be a signal for relatively slow cooling of the silicate melt (Ettler et al., 2009). The amorphous character of the studied slags is demonstrated by high background level on XRD patterns (Fig. 2). Amorphous nature of slags indicates that the cooling process was fast, which is confirmed by technology of their making. Lead slag (LS), containing the biggest number of crystallites, was cooled "naturally", meaning that it is subjected to the ambient temperature cooling on an isolated heap. On the other hand, granulated slag (GS) is quenched with water immediately after smelting, therefore it does not contain crystallites, but only droplets of metallic Cu-Pb. In case of shaft furnace slag (SFS) the melt consists of two parts: a) crystalline matte and b) glassy foam. In this study, the glassy part was examined. This was confirmed by earlier studies of crystalline part of SFS carried out by Potysz et al. (2016b), where the microscopic and chemical investigation revealed presence of crystallites such as pyroxenes, along with sulfides and intermetallic compounds. The same authors have studied similar slag samples and demonstrated that GS is texturally vitreous material with widely dispersed intermetallic inclusions. The LS samples from Dörschl furnace were studied before (Muszer, 2006). The results of the present study are in agreement with earlier results, that discovered olivines and amorphous silicate phase as main components of the slag. The study carried out by Muszer revealed that virtually all phases were non-stoichiometric. The presence of cubanite ($CuFe_2S_3$), that is another

Table 8
Concentrations of metals in leachates from EN12457 and SPLP from lead slag (LS), shaft furnace slag (SFS) and granulated slag (GS).

Concentration in leachates [mg dm^{-3}]	EN12457			SPLP		
	LS	SFS	GS	LS	SFS	GS
As	≤0.001	0.010	≤0.001	≤0.001	0.017	≤0.001
Cd	0.002	≤0.0003	0.002	0.003	≤0.0003	0.016
Cr	≤0.005	≤0.005	≤0.005	≤0.005	≤0.005	≤0.005
Cu	0.251	0.016	0.030	0.135	0.012	0.080
Pb	0.377	≤0.0001	0.031	0.225	≤0.0001	0.105
Zn	0.810	0.069	0.064	0.560	0.054	1.366

Table 7
Composition of intermetallic compounds determined in lead slag (LS), shaft furnace slag (SFS) and granulated slag (GS).

Chemical components [wt%]	Metallic Cu									Metallic Fe		
	LS (n = 4)			SFS (n = 4)			GS (n = 4)			LS (n = 4)		
	Max	Min	Average	Max	Min	Average	Max	Min	Average	Max	Min	Average
Fe	7.08	6.51	6.80	5.74	1.89	3.84	3.04	1.36	2.03	92.31	85.08	88.70
Cu	72.87	72.75	72.81	93.59	87.48	91.52	98.64	87.93	94.51	2.11	1.81	1.96
Sn	5.33	3.69	4.51	na	na	na	na	na	na	0.40	0.00	0.20
Sb	2.31	2.11	2.21	na	na	na	na	na	na	na	na	na
As	na	na	na	1.17	0.00	0.39	10.38	0.00	3.46	9.69	2.59	6.14
Cr	na	na	na	6.83	0.00	3.78	na	na	na	na	na	na
Chemical components [wt%]	Metallic Pb									Co-Ni-Fe-Cu-As alloy		
	LS (n = 9)			SFS (n = 4)			GS (n = 4)			SFS (n = 6)		
	Max	Min	Average	Max	Min	Average	Max	Min	Average	Max	Min	Average
Pb	95.41	81.96	89.28	88.90	80.73	84.82	89.76	88.69	89.11	na	na	na
Fe	10.72	3.33	6.28	6.09	4.15	5.12	1.06	1.02	1.04	44.33	6.68	17.56
Cu	3.03	0.00	1.50	13.17	5.30	9.24	10.29	9.18	9.86	9.18	3.72	7.88
Zn	6.56	0.00	2.32	1.02	0.00	0.51	na	na	na	0.58	0.00	0.10
As	0.68	0.00	0.08	0.63	0.00	0.32	na	na	na	25.34	1.71	16.66
Sb	0.32	0.00	0.06	na	na	na	na	na	na	6.68	0.00	4.09
Co	0.76	0.00	0.08	na	na	na	na	na	na	46.76	11.51	22.39
Ni	na	na	na	na	na	na	na	na	na	37.92	2.89	29.35

na – not assigned.

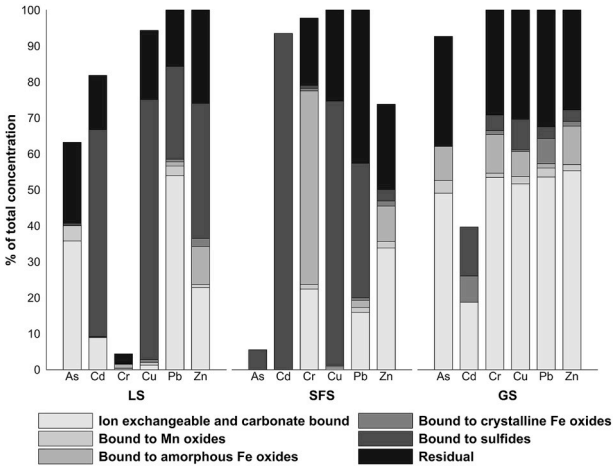

Fig. 8. Binding forms of selected elements in lead slag (LS), shaft furnace slag (SFS) and granulated slag (GS) based on sequential extraction procedures.

(next to idaite and nukundamite determined in this study) product of chalcopyrite alteration, was confirmed, which is another evidence of Cu depletion in the melt leading to formation of non-typical Cu-Fe sulfides. Another non-typical sulfide found in this study is troilite (FeS), that has also been found in Cu-Co slags from Copperbelt Province, Zambia (Vítková et al., 2010). Other than that, the slags exhibit similar phases (fayalite, spinel oxides, sulfides, intermetallic compounds) to other slags from current and historical Cu production (Sãez et al., 2003; Ettler et al., 2009; Vítková et al., 2010; Rozendaal and Horn, 2013; Potysz et al., 2016b; Khorasanipour and Esmaeilzadeh, 2016). However, comparison of our results with earlier studies on copper by-products (e.g. Kucha et al., 1998; Kucha and Cichowska, 2001) revealed that less amount of precious metals (e.g. Ag) is present in the slags from recent production, which might likely be due to development of the recovery process being applied at the present time.

Chemical composition of slags varies from one sample to another (Table 1). The reason for this is the fact that each sample is derived from a different part of the production chain. The high abundance of minor elements such as As, Cd, Cu, Ni, Pb and Zn suggests that these materials may pose threat of metal mobilization when deposited on dumps and exposed to weather conditions. The composition of studied slags displays similarities to other slags described in literature. The enrichments in Cu, Pb, Zn and other metals suggests that the concentration and smelting processes are not 100% effective. Noteworthy is the enrichment of studied materials in rare earth elements, especially in SFS and GS (255 and 308 mg kg^{-1}, respectively), particularly visible when normalized against chondritic meteorites (Fig. 1C). Other valuable elements such as Co, Mo and V are also present in high amounts (Table 2). These elements are considered scarce or critical both in European Union and Poland (Smakowski, 2011; Kamenopoulos and Agioutantis, 2012; EC, 2017). The elevated concentrations of these elements have been reported in other waste materials such as electronic waste (Müller et al., 2015; Sommer et al., 2015), municipal solid waste (Morf et al., 2013), coal fly ashes (Blissett et al., 2014), phosphogypsum (Kulczycka et al., 2016) and slags, e.g. from Fe production or bauxite residue smelting (Binnemans et al., 2015; Zimmermann and Gößling-Reisemann, 2013; Kasina and Michalik, 2016).

5.2. Metal mobility

Results of leaching both with water and simulated rainfall indicate that slags do not pose remarkable threat when exposed to environmental conditions. Values determined by ICP-MS for leachates resulting from both water and precipitation leaching exceed neither permissible levels for wastewaters nor for non-hazardous wastes (Fig. 8). However, it has to be noted that values of Cu, Pb and Zn extracted from LS were close to threshold limits. Likewise, Zn extraction from GS also approached critical concentration level. Only the amounts of extracted metals from SFS were far from these permissible levels. Therefore, based on overall extraction results, studied slags in the context of potential hazard can be ranked as follows: LS > GS > SFS. The values were also compared to national water quality criteria in United States, as performed by Piatak et al. (2004). The permissible levels of elements reported by EPA (EPA Criteria, 2018) are as follows (in μg dm^{-3}): As - 340, Cd - 1.8, Cr(III + VI) - 586, Cu - 13, Pb - 65, Zn - 120. Comparison of experimental values with the US criteria shows that the standards were met by As and Cr (in all samples and both leaching tests), by Cd and Pb in SFS sample and by Pb in GS sample. Other elements were leached in amounts exceeding the US standards for drinking water. The SPLP method seems to be more appropriate to be used in this kind of research because of the similarity to rainfall parameters (especially pH) observed nowadays. Similar results were obtained by Piatak et al. (2004) who used SPLP and water leaching protocols for historical slags; the levels of metal(loid)s in leachates did exceed acute and chronic toxicity levels for water habitats. The tests carried out in this paper were applied to the fine-grained (< 1 mm) fraction of slags. In reality, slag dumps or tailings contain larger grains of material or even solidified compact mass of slag melt. Therefore, our research represent worst-case scenario and slags from large dumps will release metals at slower rates as compared to laboratory leaching rates (Ettler et al., 2009, Vítková et al., 2011). However, the slag deposits should not be considered safe for the environment for 2 reasons: a) as every geological material, slags are susceptible to weathering, as evidenced by secondary phases abundance in slag heaps (Bril et al., 2008; Ettler et al., 2009; Potysz et al., 2015 and references therein) b) substantial amounts of metals are present in the surrounding environments nearby slag dumps or tailings exposed to prolonged weathering impact (Kierczak and Pietranik, 2011; Kierczak et al., 2013).

Sequential extraction performed in six steps shows that some metals can be released to the environment in considerable amounts (Fig. 8). Granulated slag contains metals in easily or moderately mobile forms to the greatest extent among tested materials. On the other hand, slags such as SFS and LS are rich in metals that are less labile. In all cases, the amounts of metals extracted in certain steps are associated with chemistry of mineral phases.

Crystalline spinels from LS sample were not dissolved, which is reflected by very low amount of dissolved Cr. In LS sample, Zn is extracted partially as exchangeable fraction due to its abundance in glass (up to 8.75 wt%), as well as in olivines (up to 5.14 wt%). The occurrence of Cu and Zn in sulfidic fraction is linked to their abundance as nukundamite and sphalerite and the presence in pyrrhotite (Table 6). The Fe-oxide fraction of Zn is presumably tied to dissolution of glass and olivines, that contain some amounts of Zn (Table 3, Table 4). The reason of high Pb abundance as exchangeable and sulfide-bound fractions is more difficult to explain. Presumably, the reason of such phenomenon is gradual dissolution of metallic Pb inclusions by subsequent extracting agents. This might also be an explanation of As abundance in exchangeable fraction, along with dissolution of metallic Fe, that are main carriers of As in LS. The occurrence of Cd as sulfide-bound and exchangeable is also tied to this, because Cd occurs solely in metallic Pb. The high susceptibility to dissolution of metallic phases in slags has been confirmed in the previous studies (Ettler et al., 2002; Potysz et al., 2018c).

In case of SFS, As and Cd were bound to sulfidic fraction (F5) since the only appearance of those constituents is in sphalerite. It must be noted that the volumetric content of sphalerite in SFS is small, and for this reason Zn was extracted in low amount in sulfide fraction, although sphalerite is main Zn-bearing mineral. This might be an explanation for incomplete dissolution of these (As, Cd) elements. On the other hand, Cu, which is also present mainly in idaite (sulfide), has been extracted totally, with 74% of it being bound to sulfides. This might be a signal that idaite is more susceptible to leaching than sphalerite. The presence of Pb in the sulfidic fraction is probably another misleading

information, because no Pb is abundant in sulfide phases from SFS (Table 6). For that reason, F5 fraction of Pb should be probably accounted to residual part, that presumably is a result of dissolution of metallic Pb inclusions. An easy dissolution of metallic Pb has already been reported (Potysz et al., 2016b). The dissolution of Cr in amorphous Fe oxide fraction (F3) may be a result of dissolution of the spinel-containing glass matrix. The spinels (a main Cr-bearing phase) in SFS are found as inclusions in glass and not the well-formed crystals, which might be a reason of their susceptibility to dissolution.

Most of metals released from GS were associated with F1 fraction - extraction by acetic acid, which has been recognized as complexing agent, causing enhanced metal release as compared to less aggressive reagents (Hass and Fine, 2010). Some of metals are also bound to Mn-Fe oxides, that are a component of glassy matrix of GS. The presence of the sulfidic fraction in the overall metals leached from GS is probably a glitch, since no sulfides are present in the GS sample, and this fraction should be probably accounted to Mn-Fe oxides part.

As proven by our study, results of sequential extraction show that this procedure might be inadequate in some cases, especially in case of mineralogically complex waste materials, because the dissolved fractions might mix with each other (Hass and Fine, 2010). Regardless, findings from sequential extractions can be useful during investigating of the effects of weathering on stored mineral wastes (Jerzykowska et al., 2014). Undoubtedly, it has to be pointed out that laboratory leaching rates do not reflect exact dissolution rates encountered in the field. The latter are slower as compared to the laboratory rates. This is because weathering factors of different strength occur simultaneously in the field. It is known that some weathering agents (e.g. organic acids, microbial activity and others) enhance the rate of weathering, whereas others counteract the process (e.g. secondary phases formation, metal sorption on soil particles). Thus, these processes acting together undoubtedly modify the real weathering rates through hindering or facilitating migration of elements depending on the actual conditions faced. Therefore, lab-scale extractions are being used for general wastes characterization in terms of their susceptibility to release out the toxic elements and often represent so-called worst-case scenario.

6. Conclusions

In this study, we examined three different slag residues derived from Cu production in SW Poland. Leaching protocols applied to assess the environmental stability of examined materials revealed that simulated rainfall leads to negligible metal(loid) discharge in the view of the worst-case scenario. On the other hand, sequential extraction results indicate that the metals are not bound to labile fractions unless the material is highly amorphous (GS). Nonetheless, the results of this study demonstrated that studied slags are susceptible to release out metals. Therefore, further focus of this research should be placed on metal recovery feasibility studies. The high concentrations of valuable metals considered critical or scarce (REE, Co, Mo, V) in slags combined with their dubious environmental stability can be seen as an imperative to conduct further research concerning the efficient recovery of metals from these slags. The recovery can be achieved using environment-friendly methods, e.g. bioleaching, which is currently being performed by our team. Since sulfuric acid has been one of the most frequently studied extracting agent proven to perform efficient extraction, an application of H_2SO_4 will be done. Furthermore, H_2SO_4 can also be biologically produced (Oliveira et al., 2013). Thus, biologically assisted metals extraction is a “green” alternative to the chemical leaching. On the other hand, organic extractants are also known for their good performance due to complexing features. Thus, a comparison between inorganic and organic leaching, as well as chemical versus biological leaching, will be attempted as the next steps of our studies.

Funding

This research has been funded by AGH University of Science and Technology - Statutory Research [Project No. 15.11.140.003] to BM and by National Science Centre in Poland - FUGA grant [UMO-2016/20/S/ST10/00545] to AP.

Acknowledgements

The authors would like to acknowledge Mr Adam Gaweł for help in XRD and SEM analyzes and Mr Wiesław Knap for performing ICP-MS analyzes. The authors would also like to express their thanks to one anonymous reviewer and to Prof. Hubert Bril for their professional and valuable comments that helped to improve the quality and clarity of the manuscript.

Appendix A. Supplementary data

Supplementary data to this article can be found online at https://doi.org/10.1016/j.apgeochem.2018.11.017.

References

Bau, M., 1991. Rare-earth element mobility during hydrothermal and metamorphic fluid-rock interaction and the significance of the oxidation state of europium. Chem. Geol. 93 (3–4), 219–230.

Binnemans, K., Jones, P.T., Blanpain, B., Van Gerven, T., Yang, Y., Walton, A., Buchert, M., 2013. Recycling of rare earths: a critical review. J. Clean. Prod. 51, 1–22.

Binnemans, K., Jones, P.T., Blanpain, B., Van Gerven, T., Pontikes, Y., 2015. Towards zero-waste valorisation of rare-earth-containing industrial process residues: a critical review. J. Clean. Prod. 99, 17–38.

Blissett, R.S., Smalley, N., Rowson, N.A., 2014. An investigation into six coal fly ashes from the United Kingdom and Poland to evaluate rare earth element content. Fuel 119, 236–239.

Bril, H., Zainoun, K., Puziewicz, J., Courtin-Nomade, A., Vanaecker, M., Bollinger, J.-C., 2008. Secondary phases from the alteration of a pile of zinc-smelting slag as indicators of environmental conditions: an example from Świętochłowice, Upper Silesia, Poland. Can. Mineral. 46 (5), 1235–1248.

Du, X., Graedel, T.E., 2011. Global in-use stocks of the rare earth elements: a first estimate. Environ. Sci. Technol. 45 (9), 4096–4101.

Du, X., Graedel, T.E., 2013. Uncovering the end uses of the rare earth elements. Sci. Total Environ. 461–462, 781–784.

EC, 2017. Communication from the commission to the European parliament, the council, the European economic and social committee and the committee of the regions on the 2017 list of critical raw materials for the EU. https://eur-lex.europa.eu/legal-content/EN/TXT/PDF/?uri=CELEX:52017DC0490&from=EN.

EN 12457-2 2002. Characterisation of Waste - Leaching - Compliance Test for Leaching of Granular Waste Materials and Sludges - Part 2: One Stage Batch Test at a Liquid to Solid Ratio of 10 L/kg for Materials with Particle Size below 4 mm (Without or with Size Reduction).

EPA Criteria, 2018. National recommended water quality criteria - aquatic life criteria table. https://www.epa.gov/wqc/national-recommended-water-quality-criteria-aquatic-life-criteria-table#table.

Ettler, V., Mihaljevič, M., Touray, J.-C., Piantone, P., 2002. Leaching of polished sections: an integrated approach for studying the liberation of heavy metals from lead-zinc metallurgical slags. Bull. Soc. Geol. Fr. 173, 161–169.

Ettler, V., Johan, Z., Kříbek, B., Šebek, O., Mihaljevič, M., 2009. Mineralogy and environmental stability of slags from the Tsumeb smelter, Namibia. Appl. Geochem. 24, 1–15.

Evensen, N.M., Hamilton, P.J., O'Nions, R.K., 1978. Rare-earth abundances in chondritic meteorites. Geochim. Cosmochim. Acta 42 (8), 1199–1212.

Goodenough, K.M., Schilling, J., Jonsson, E., Kalvig, P., Charles, N., Tuduri, J., Deady, E.A., Sadeghi, M., Schiellerup, H., Müller, A., Bertrand, G., Arvanitidis, N., Eliopoulos, D.G., Shaw, R.A., Thrane, K., Keulen, N., 2016. Europe's rare earth element resource potential: an overview of REE metallogenetic provinces and their geodynamic setting. Ore Geol. Rev. 72 (1), 838–856.

Gorai, B., Jana, R.K., Premchand, 2003. Characteristics and utilisation of copper slag - a review. Resour. Conserv. Recycl. 39 (4), 299–313.

Gromet, L.P., Haskin, L.A., Korotev, R.L., Dymek, R.F., 1984. The “North American shale composite”: its compilation, major and trace element characteristics. Geochim. Cosmochim. Acta 48 (12), 2469–2482.

Hass, A., Fine, P., 2010. Sequential selective extraction procedures for the study of heavy metals in soils, sediments, and waste materials - a critical review. Crit. Rev. Environ. Sci. Technol. 40 (5), 365–399.

ISO 17294-2:2016. “Water Quality – Application of Inductively Coupled Plasma Mass Spectrometry (ICP-MS) – Part 2: Determination of Selected Elements Including Uranium Isotopes”.

Jarošíková, A., Ettler, V., Mihaljevič, M., Kříbek, B., Mapani, B., 2017. The pH-dependent leaching behavior of slags from various stages of a copper smelting process:

environmental implications. J. Environ. Manag. 187, 178–186.
Jerzykowska, I., Majzlan, J., Michalik, M., Göttlicher, J., Steininger, R., Błachowski, A., Ruebenbauer, K., 2014. Mineralogy and speciation of Zn and as in Fe-oxide-clay aggregates in the mining waste at the MVT Zn–Pb deposits near Olkusz, Poland. Chem. Erde-Geochem. 74 (3), 393–406.
Kabata-Pendias, A., Szteke, B., 2015. Trace Elements in Abiotic and Biotic Environments. CRC Press, Taylor&Francis Group, New York.
Kaksonen, A.H., Särkijärvi, S., Puhakka, J.A., Peuraniemi, E., Junnikkala, S., Tuovinen, O.H., 2017. Solid phase changes in chemically and biologically leached copper smelter slag. Miner. Eng. 106, 97–101.
Kamenopoulos, S.N., Agioutantis, Z., 2012. Rare earth elements: a review and analysis of their multi-dimensional global importance. Cuprum 3 (64), 45–59.
Kasina, M., Michalik, M., 2016. Iron metallurgy slags as a potential source of critical elements - Nb, Ta and REE. Mineralogia 48 (1–2), 15–28.
Kersten, M., Förstner, U., 1986. Chemical fractionation of heavy metals in anoxic estuarine and coastal sediments. Water Sci. Technol. 18 (4–5), 121–130.
Khorasanipour, M., Esmaeilzadeh, E., 2016. Environmental characterization of Sarcheshmeh Cu-smelting slag, Kerman, Iran: application of geochemistry, mineralogy and single extraction methods. J. Geochem. Explor. 166, 1–17.
Kierczak, J., Pietranik, A., 2011. Mineralogy and composition of historical Cu slags from the Rudawy Janowickie Mountains, southwestern Poland. Can. Mineral. 49 (5), 1281–1296.
Kierczak, J., Potysz, A., Pietranik, A., Tyszka, R., Modelska, M., Néel, C., Ettler, V., Mihaljevič, M., 2013. Environmental impact of the historical Cu smelting in the Rudawy Janowickie Mountains (south-western Poland). J. Geochem. Explor. 124, 183–194.
Kozłowska-Roman, A., Oszczepalski, S., 2016. Polish Copper & Silver. https://doi.org/10.13140/RG.2.2.18654.84802. (in Polish).
Kua, H.W., 2013. The consequences of substituting sand with used copper slag in construction. J. Ind. Ecol. 17, 869–879.
Kucha, H., Piestrzyński, A., Cichowska, R., Rajchel, B., 1998. Mineralogical and chemical research of copper metallurgy by-products. Polskie Towarzystwo Mineralogiczne – Prace Specjalne 10, 201–219 (in Polish).
Kucha, H., Cichowska, R., 2001. Precious metals in copper smelting products. Physicochem. Probl. Miner. Process 35, 91–101. http://www.journalssystem.com/ppmp/Precious-metals-in-copper-smelting-products,79574,0,2.html.
Kucha, H., 2003. Geology, mineralogy and geochemistry of the Kupferschiefer, Poland. In: Kelly, J.G. (Ed.), Europe's Major Base Metal Deposits. Irish Association for Economic Geology, Dublin.
Kulczycka, J., Kowalski, Z., Smol, M., Wirth, H., 2016. Evaluation of the recovery of rare earth elements (REE) from phosphogypsum waste – case study of the WIZÓW chemical plant (Poland). J. Clean. Prod. 113, 345–354.
Lackovic, J.A., Nikolaidis, N.P., Chheda, P., Carley, R.J., Patton, E., 1997. Evaluation of batch leaching procedures for estimating metal mobility in glaciated soils. Ground Water Monit. R. 17, 231–240.
Lottermoser, B.G., 2005. Evaporative mineral precipitates from a historical smelting slag dump, Rio Tinto, Spain. N. Jb. Miner. Abh. 181 (2), 183–190.
Morf, L.S., Gloor, R., Haag, O., Haupt, M., Skutan, S., Di Lorenzo, F., Böni, D., 2013. Precious metals and rare earth elements in municipal solid waste – sources and fate in a Swiss incineration plant. Waste Manag. 33 (3), 634–644.
Müller, S.R., Wäger, P.A., Widmer, R., Williams, I.D., 2015. A geological reconnaissance of electrical and electronic waste as a source for rare earth metals. Waste Manag. 45, 226–234.
Murari, K., Siddique, R., Jain, K.K., 2015. Use of waste copper slag, a sustainable material. J. Mater. Cycles Waste 17 (1), 23–26.
Muszer, A., 2006. Petrographical and mineralogical characteristics of the metallurgical slag from the Dörschl furnace (Głogów foundry, Poland). Physicochem. Probl. Miner. Process. 40, 89–98.
Oliveira, D.M., Sobral, L.G.S., Rocha, P.M., Padrão, D.O., 2013. Biological generation of sulphuric acid for bioleaching of copper oxide ores. In: XXV Encontro Nacional de Tratamento de Minérios e Metalurgia Extrativa & VIII Meeting of the Southern Hemisphere on Mineral Technology, Goiânia - GO, 20 a 24 de Outubro 2013.
Oszczepalski, S., Chmielewski, A., Mikulski, S., 2016. Controls on the distribution of rare earth elements in the Kupferschiefer series of SW Poland. Geol. Q. 60 (4), 811–826.
Paulick, H., Machacek, E., 2017. The global rare earth element exploration boom: an analysis of resources outside of China and discussion of development perspectives. Resour. Pol. 52, 134–153.
Piatak, N.M., Seal II, R.R., Hammarstrom, J.M., 2004. Mineralogical and geochemical controls on the release of trace elements from slag produced by base- and precious-metal smelting at abandoned mine sites. Appl. Geochem. 19 (7), 1039–1064.
Piatak, N.M., Parsons, M.B., Seal II, R.R., 2015. Characteristics and environmental aspects of slag: a review. Appl. Geochem. 57, 236–266.
Potysz, A., van Hullebusch, E.D., Kierczak, J., Grybos, M., Lens, P.N.L., Guibaud, G., 2015. Copper metallurgical slags - current knowledge and fate: a review. Crit. Rev. Environ. Sci. Technol. 45 (22), 2424–2488.
Potysz, A., Grybos, M., Kierczak, J., Guibaud, G., Lens, P.N.L., van Hullebusch, E.D., 2016a. Bacterially-mediated weathering of crystalline and amorphous Cu-slags. Appl. Geochem. 64, 92–106.
Potysz, A., Kierczak, J., Fuchs, Y., Grybos, M., Guibaud, G., Lens, P.N.L., van Hullebusch, E.D., 2016b. Characterization and pH-dependent leaching behaviour of historical and modern copper slags. J. Geochem. Explor. 160, 1–15.
Potysz, A., Grybos, M., Kierczak, J., Guibaud, G., Fondaneche, P., Lens, P.N.L., van Hullebusch, E.D., 2017. Metal mobilization from metallurgical wastes by soil organic acids. Chemosphere 178, 197–211.
Potysz, A., van Hullebusch, E.D., Kierczak, J., 2018a. Perspectives regarding the use of metallurgical slags as secondary metal resources - a review of bioleaching approaches. J. Environ. Manag. 219, 138–152.
Potysz, A., Kierczak, J., Grybos, M., Pedziwiatr, A., van Hullebusch, E.D., 2018b. Weathering of historical copper slags in dynamic experimental system with rhizosphere-like organic acids. J. Environ. Manag. 222, 325–337.
Potysz, A., Kierczak, J., Pietranik, A., Kądziołka, K., 2018c. Mineralogical, geochemical, and leaching study of historical Cu-slags issued from processing of the Zechstein formation (Old Copper Basin, southwestern Poland). Appl. Geochem. 98, 22–35. https://doi.org/10.1016/j.apgeochem.2018.08.027.
Puziewicz, J., Zainoun, K., Bril, H., 2007. Primary phases in pyrometallurgical slags from a zinc-smelting waste dump, Świętochłowice, Upper Silesia, Poland. Can. Mineral. 45, 1189–1200.
Rice, C.M., Atkin, D., Bowles, J.F.W., Criddle, A.J., 1979. Nukundamite, a new mineral, and idaite. Miner. Mag. 43, 193–200.
RME, 2014. Regulation of the Ministry of the Environment of 18 November 2014 on the Conditions to Be Met as Regards the Release of Sewage into the Water or onto the Land and on the Substances, that Are Particularly Harmful to the Aquatic Environment (Off. Gazette 2014, Item 1800). (in Polish).
RMEc, 2015. Regulation of the Ministry of the Economics on the Conditions to Be Met as Regards the Admittance of Waste to Be Deposited on Landfills (Off. Gazette 2015, Item 1277). (in Polish).
Rozendaal, A., Horn, R., 2013. Textural, mineralogical and chemical characteristics of copper reverb furnace smelter slag of the Okiep Copper District, South Africa. Miner. Eng. 52, 184–190.
Sāez, R., Nocete, F., Nieto, J.M., Capitān, M.A., Rovira, S., 2003. The extractive metallurgy of copper from Cabezo Jurē, Huelva, Spain: chemical and mineralogical study of slags dated to the third millennium B.C. Can. Mineral. 41, 627–638.
Sawłowicz, Z., 2013. REE and their relevance to the development of the Kupferschiefer copper deposit in Poland. Ore Geol. Rev. 55, 176–186.
Sawłowicz, Z., Sutton, S., 2017. Uwagi na temat geochemii łupka miedzionośnego z monokliny przedsudeckiej. In: Kowalczuk, P.B., Drzymała, J. (Eds.), Łupek Miedzionośny III. WGGG PWr, Wrocław, https://doi.org/10.5277/lupek1701. (in Polish).
Schulze, R., Buchert, M., 2016. Estimates of global REE recycling potentials from NdFeB magnet material. Resour. Conserv. Recycl. 113, 12–27.
Shi, C., Meyer, C., Behnood, A., 2008. Utilization of copper slag in cement and concrete. Resour. Conserv. Recycl. 52, 1115–1120.
Smakowski, T.J., 2011. Critical or Deficit Mineral Commodities for EU and Poland Economy, vol. 81. The Bulletin of The Mineral and Energy Economy Research Institute of the Polish Academy of Sciences, pp. 59–68 (in Polish, with English summary).
Sommer, P., Rotter, V.S., Ueberschaar, M., 2015. Battery related cobalt and REE flows in WEEE treatment. Waste Manag. 45, 298–305.
Szymański, A., 1989. Technical Mineralogy and Petrography: an Introduction to Materials Technology. Elsevier, New York.
Taylor, S.R., 1964. Abundance of chemical elements in the continental crust: a new table. Geochem. Cosmochim. Acta 28, 1273–1285.
Taylor, S.R., McLennan, S.M., 1985. The Continental Crust; Its Composition and Evolution; an Examination of the Geochemical Record Preserved in Sedimentary Rocks. Blackwell, Oxford.
Tyszka, R., Pietranik, A., Kierczak, J., Zieliński, G., Darling, J., 2018. Cadmium distribution in Pb-Zn slags from Upper Silesia, Poland: implications for cadmium mobility from slag phases to the environment. J. Geochem. Explor. 186, 215–224.
US EPA, 1994. Method 1312. Synthetic precipitation leaching procedure. In: SW-846: Test Methods for Evaluating Solid Waste. Physical/Chemical Methods. Office of Solid Waste, Washington, DC, USA, . https://www.epa.gov/sites/production/files/2015-12/documents/1312.pdf/.
USGS, 2018. Copper. https://minerals.usgs.gov/minerals/pubs/commodity/copper/mcs-2018-coppe.pdf.
Vandenberghe, R.E., de Resende, V.G., da Costa, G.M., De Grave, E., 2010. Study of loss-on-ignition anomalies found in ashes from combustion of iron-rich coal. Fuel 89 (9), 2405–2410.
Vítková, M., Ettler, V., Johan, Z., Kříbek, B., Šebek, O., Mihaljevič, M., 2010. Primary and secondary phases in copper-cobalt smelting slags from the Copperbelt Province, Zambia. Miner. Mag. 74 (4), 581–600.
Vítková, M., Ettler, V., Mihaljevič, M., Šebek, O., 2011. Effect of sample preparation on contaminant leaching from copper smelting slag. J. Hazard Mater. 197, 417–423.
Warchulski, R., Gawęda, A., Kądziołka-Gaweł, M., Szopa, K., 2015. Composition and element mobilization in pyrometallurgical slags from the Orzeł Biały smelting plant in the Bytom-Piekary Śląskie area. Poland. Mineral. Mag. 79 (2), 459–483.
Whitney, D.L., Evans, B.W., 2010. Abbreviations for names of rock-forming minerals. Am. Mineral 95 (1), 185–187.
Winchell, A.N., Winchell, H., 1964. The Microscopical Characters of Artificial Inorganic Solid Substances: Optical Properties of Artificial Minerals. Academic Press, New York.
Wu, W., Zhang, W., Ma, G., 2010. Optimum content of copper slag as a fine aggregate in high strength concrete. Mater. Des. 31, 2878–2883.
Zimmermann, T., Gößling-Reisemann, S., 2013. Critical materials and dissipative losses: a screening study. Sci. Total Environ. 461–462, 774–780.